MEDWIN PUBLISHERS
Committed to create value for Researchers

International Journal of Biochemistry & Physiology

Pre-Steady-State Kinetics of the Binding and Hydrolysis of mant-cGMP by Phosphodiesterase-5

Morris GZ[1]*, Ke H[2], Wang H[2], Francis SH[3], Corbin JD[3], Belknap B[4] and White HD[4]

[1]Department of Science and Mathematics, Glenville State College, USA

[2]Department of Biochemistry and Biophysics and Lineberger Comprehensive Cancer Center, University of North Carolina, USA

[3]Department of Molecular Physiology and Biophysics, Vanderbilt University School of Medicine, USA

[4]Department of Physiological Sciences, Eastern Virginia Medical School, USA

***Corresponding author:** Gary Z Morris, Department of Science and Mathematics, Glenville State College, Glenville, West Virginia 26351, USA, E-mail: gary.morris@glenville.edu

Research Article

Volume 1 Issue 1

Received Date: August 17, 2016

Published Date: August 26, 2016

Abstract

Phosphodiesterase-5 (PDE5), receptor for the drugs sildenafil (Viagra®), vardenafil (Levitra®), and tadalafil (Cialis®), selectively hydrolyzes the second messenger cGMP. However, its hydrolytic mechanism is unknown. The hydrolyzable substrate analog mant-cGMP and isolated PDE5 catalytic domain were used to study substrate interaction and subsequent hydrolysis. Stopped-flow analysis by Förster/fluorescence resonance energy transfer (PDE5 tryptophans →mant-cGMP) identified five steps. The rate constant of mant-cGMP binding to PDE5 catalytic domain was measured to be 2.4 x 10^7 M^{-1} s^{-1} at 4°C but was too rapid to be measured at 20°C. Substrate binding was followed by two additional Mg^{2+}-dependent, and mant-cGMP concentration-independent increases in fluorescence (Steps 2 and 3). The decrease in fluorescence that occurred with Step 4 had the same rate as the hydrolytic step measured by quench-flow and was attributed to be hydrolysis followed by rapid product dissociation. These results suggested that hydrolysis of mant-cGMP is the rate-limiting step of the enzymatic reaction and that the final slow increase in fluorescence is due to the binding of nonenzymatically isomerized product, mant-5'-GMP (2'→3') to the enzyme. We propose a model whereby mant-cGMP in the presence of Mg^{2+} rapidly binds to the catalytic site of the enzyme, followed by multi-step formation of increasingly tight enzyme-substrate complexes prior to mant-cGMP hydrolysis and rapid dissociation of the product, mant-5'-GMP.

Keywords: Phosphodiesterase-5 (PDE5); mant-cGMP; Pre-steady-state; TLC; FRET

Abbreviations: C domain: Isolated catalytic domain of phosphodiesterase-5; E- Enzyme; EDTA: Ethylene diamine tetra acetic acid; mant: 2'-O-N-methylanthraniloyl; P: Product; PDE: Phospho diesterase; S: Substrate; TLC: Thin layer chromatography

Introduction

Because cyclic nucleotide phosphodiesterases (PDEs) modulate cellular cyclic nucleotide levels, catalytic activities of PDEs are critical in regulating many physiological processes. Based on natural selection it can be surmised that PDEs catalyze cyclic nucleotide breakdown at a rate that modulates their levels within a range that is appropriate for physiological responses in a particular cell type or cellular compartment [1-6]. For example, PDE6 in retinal photoreceptors can turn over the total pool of cGMP within ~0.015 sec following a moderate light flash; this leads to generation of a signal that is perceived by central nerves [1]. The rapid rate of cGMP hydrolysis in photoreceptors can be contrasted with that in vascular smooth muscle cells, where cGMP elevated in response to nitrous oxide is turned over by PDE5 in ~50 sec [2], thus allowing for restoration of cellular Ca^{2+}. A number of studies have investigated aspects of the catalytic mechanism of various PDEs [7-16] but the precise molecular steps that occur during binding and hydrolysis of cyclic nucleotide and the subsequent dissociation of the 5'-nucleotide product are unknown. Here in we use purified recombinant isolated human PDE5 C domain, the fluorescent substrate analog2'-O-(N-methylanthraniloyl)-cGMP (2'-mant-cGMP, mant-cGMP), and the fluorescent product analog 2'-O-(N-methylanthraniloyl)-5'-GMP (mant-5'-GMP) (Figure 1), to study the catalytic mechanism of PDE5.

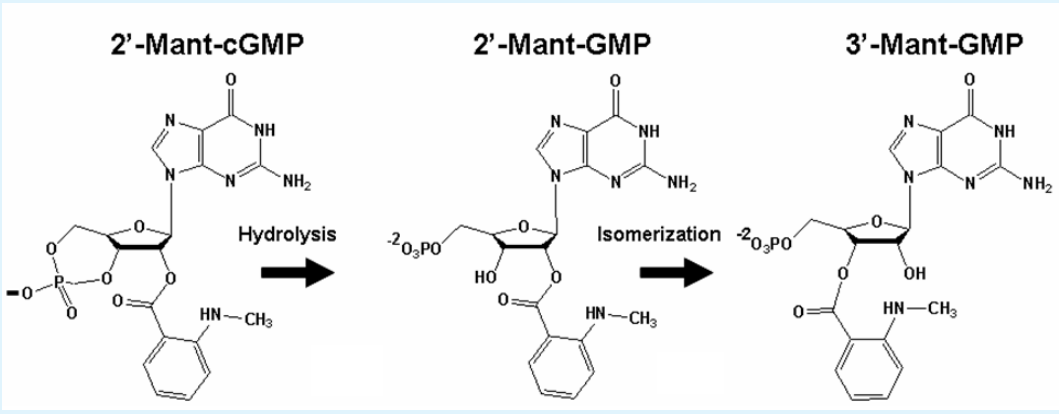

Figure 1: Chemical structures of 2'-*O*-(*N*-methylanthraniloyl)-cGMP (2'-mant-cGMP, mant-cGMP) and the products [2'- mant-5'-GMP (2'-mant-GMP) and 3'-mant-5'-GMP (3'-mant-GMP)] of PDE5 hydrolysis.

Experimental Procedures

Materials

mant-cGMP and mant-5'-GMP were either purchased from Biolog (Life Science Institute, Germany) or synthesized as described below. QAE-Sephadex, EDTA, theophylline, bovine serum albumin, histonetype II-AS, *Crotalus atrox* snake venom 5'-nucleotidase, 5'-5'-GMP (GMP), cGMP, $MgCl_2$, $Mg(C_2H_3O_2)$, Tris base, and solvents were obtained from Sigma-Aldrich (St. Louis, MO USA). *N*-methylisatoic anhydride, was obtained from Invitrogen-Molecular Probes (Carlsbad, CAUSA). Cellulose and silica gel (DC-Platikfolien Kiselgel) TLC plates (20 x 20 cm) were obtained from Kodak (Rochester, NYUSA) or Merck (Germany), respectively. [^{3}H]cGMP, Sephadex LH-20 and Sephadex G-25 resins were from Amersham Pharmacia Biotech (GEHealthcare, Little Chalfont, Buckinghamshire, UK).

Preparation of mant-analogs

mant-cGMP was purchased and synthesized from cGMP and N-methylisatoic anhydride according to the procedure of Hiratsuka (3). Both commercial and synthesized Mant-analogs were analyzed on TLC as previously described (3) and the R_f for each nucleotide was determined from the ratio of the distance traveled by the sample to that of the distance traveled by the solvent front.

Isolated PDE5 C domain

The isolated human PDE5A1 C domain (amino acids 535-860) was constructed, purified, and characterized as previously described (4,5). A portion of one of the preparations was purified in the absence of added Mg^{2+}, thus providing a stock of Mg^{2+}-free isolated PDE5 C domain. The specific enzyme activity of this preparation was comparable to that of enzyme purified in the presence of Mg^{2+} as determined in a standard PDE assay done in the presence of Mg^{2+} (see method for steady-state kinetic measurements below).

Steady-state kinetic measurements

Standard PDE activity assays were performed as described previously [5,6] to determine the IC_{50} of the two Mant-nucleotide analogs for the isolated PDE5 C domain. To demonstrate the characteristics of mant-cGMP as a substrate for the PDE5 C domain, several kinetic constants of mant-cGMP were initially determined and compared to those of cGMP. Affinities for mant-cGMP and cGMP were compared by measuring apparent inhibition of increasing concentrations of these nucleotides in a standard PDE assay under initial rate conditions and containing 0.1 micromolar [^{3}H]cGMP as substrate, which is far below the known K_m value. mant-cGMP (1 mM) was tested for hydrolysis by PDE5 C domain (0.5 µM) using overnight incubation at room temperature in the standard PDE reaction mixture. The reaction was terminated by heating samples in boiling water for 5 min; nucleotides in the reaction were resolved by two different forms of TLC, and visualized using a hand-held UV lamp. Aliquots of the reaction mixture were spotted onto both silica gel and cellulose TLC plates alongside mant-cGMP and mant-5'-GMP standards and developed.

Pre-Steady-state kinetic measurements

Stopped-flow and quench-flow were used for rapid kinetic measurement of the interaction between mant-cGMP and the PDE5 C domain. Stopped-flow was used to determine the rate of binding of mant-cGMP to isolated C domain, rate of steps subsequent to mant-cGMP binding and Mg^{2+} dependence of each step. Four tryptophans in the PDE5 C domain are located within 2 nm of the substrate-binding site (PDB code number = 1rkp). The close proximity of tryptophan side chains in the cGMP binding site suggests that FRET is likely to occur between the C domain tryptophans and mant-cGMP. For FRET to occur, the excited donor fluorophore (PDE5 tryptophans) must be located within <10 nm of the acceptor fluorophore mant-cGMP.

Previous studies have shown the importance of Mg^{2+} in the catalytic mechanism of PDE5. We have therefore determined whether Mg^{2+} is required for interaction of mant-cGMP with the C domain measured by FRET. The reaction was done with the purified enzyme in the presence of EDTA (to remove trace amounts of divalent cations that may have carried over from purification of the C domain), and in the presence or absence of added Mg^{2+}. There was only a small time-dependent increase in FRET if mant-cGMP was mixed with PDE5 without added Mg^{2+} (Figure 2). The small change in fluorescence intensity was eliminated when enzyme was mixed with mant-cGMP in the presence of EDTA and significantly increased in the presence of added Mg^{2+} (Figure 2). The fluorescence signal did not depend upon the order of addition of Mg^{2+} and mant-cGMP to enzyme.

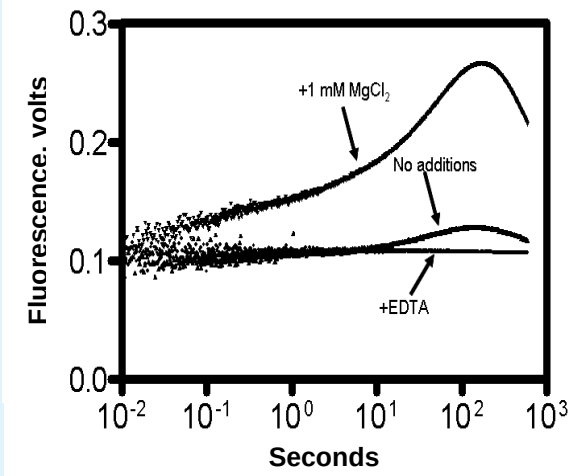

Figure 2: Requirement of Mg^{2+} for FRET between PDE5 and mant-cGMP. PDE5 C domain (2.5 µM) was pre-mixed in stopped-flow cell at 20°C with buffer (20 mM Tris-HCl, pH 7.5, 50 mM NaCl) containing either 0 mM $MgCl_2$; 5 mM EDTA; or 1 mM $MgCl_2$ for 60 sec. mant-cGMP (1.25 µM) was then added and FRET was measured with stopped-flow fluorometer, λ_{exc} = 290 nm, $\lambda_{emission}$> 420 nm.

Stopped-flow fluorescence was measured using aKinTek SF-2001 double mixing stopped-flow fluorometer. The excitation light from a 75-watt xenon lamp was selected using a 0.2 monochromator (PTI Inc.). The mixing time of the instrument was < 2 msec. Kinetic measurements of Mant-cGMP interaction with C domain were observed via fluorescence by Förster/fluorescence resonance energy transfer (FRET) using an excitation of 295 nm and emission >420 nm with a sharp cutoff filter. The KinTek stopped-flow apparatus was fitted with 2-ml

syringes in positions A and B and a 5-ml syringe in position C.

Single mixing stopped-flow experiments were performed by mixing isolated C domain in 50 mM Tris-HCl, pH 7.5, 20 mM NaCl (position A) with Mant-cGMP in the same buffer and varying concentrations of $MgCl_2$ (position C). Dilution of the syringe content was 2/7 for isolated C domain and 5/7 for Mant-cGMP. Double-mixing experiments were performed by first mixing C domain (position A) with Mant-cGMP or Mant-5'-GMP (position B), holding in a delay line for a prescribed period of time, and then mixing (chasing) with cGMP (syringe position C) to prevent rebinding of the fluorescence substrate and products to the enzyme. Dilution of the syringe content in double mixing experiments was 2/9 for isolated C domain and Mant-cGMP (positions A and B, respectively) and 5/9 for cGMP or vardenafil (position C).

Three to four data traces of 500-1000 points were averaged, and the observed rate constants (k) and amplitudes (A) were obtained by fitting the data for change in fluorescence (F) as a function of time (t) to up to five exponential terms using the following exponential equation:

$$F(t) = [\sum_{i=n}(A_i \bullet e^{(-ki \bullet t)})] + C \qquad (2)$$

Where i = index of summation, n = the number of exponential terms used to fit the data, e = the base of the natural logarithm, and C = a constant. Data calculation and analysis were done using the software package included with the KinTek stopped-flow instrument or using the least square and simplex minimization routines in the Scientist package for global fitting (MicroMath). Similar values and errors were obtained with both sets of software.

Chemical quench measurements for the hydrolysis of mant-cGMP were done by manual mixing or by using a rapid chemical quench device employing the mixing block of a KinTek quench-flow and a custom-made stepper motor drive [17]. 15 µl of isolated PDE5 C domain and 10 µl nucleotide mant-cGMP or cGMP were mixed, held in a delay line for the indicated time and quenched with 0.48 ml quench solution (30 mM KH_2PO_4 and 10 mM tetrabutyl ammonium hydroxide, pH 2.65). Acetonitrile was then added to samples for a final concentration of 30% (v/v) in samples containing mant-cGMP or 10% (v/v) in samples containing cGMP. Samples (100 µl) were loaded onto a reverse-phase chromatography column (Beckman Ultrasphere ODS column) and eluted isocratically with buffer containing the same composition as sample buffer at a flow rate of 1 ml/s. mant-cGMP and products were measured using a MacPherson 750-03 fluorescence detector equipped with a 200 watt Hg/Xe lamp. Excitation at 363 nm was selected with a monochromator and emission >420 nm was measured using a high-pass cut-off filter. Both cGMP and 5'-GMP were detected by absorption at 253 nm with a SSI 500 UV/visible detector. Voltage outputs from both detectors were recorded on a PC using a Picolog ADC-16 A/D converter with the data logging software provided by the manufacturer. The percent of nucleotide hydrolysis was determined from the areas under the fluorescence or absorption curves using software written in the laboratory of Howard White.

Statistical analyses

Measured values (n) are presented as mean ± standard error of the mean (S.E.M).

Free Mg^{2+} was calculated from $[Mg_{free}] = [Mg_{total}] - [EDTA]$ under the conditions of these experiments where $pK_{Mg} \sim 6$ (at pH 8.0) and $[Mg_{total}]$ is > 1 mM.

Results

Steady-state Kinetics of mant-cGMP as Substrate for the Isolated Human PDE5 C domain

mant-modified nucleotides have been used to study many reactions involving nucleotides because they are hydrolyzable substrate analogs in which the fluorescence emission is often sensitive to the environment when the nucleotides are bound to the active site of the enzyme [3,9]. Mant-cGMP, like cGMP, can assume the *anti*-conformation, which is the preferred conformation of cGMP for hydrolysis by PDE5 [10]. These features suggest that mant-cGMP might be an appropriate fluorescent cGMP analog to study the catalytic mechanism of PDE5. mant-cGMP has previously been characterized as a substrate for PDE1 and PDE6 [11,13] through steady-state kinetic measurements. The apparent fifty percent inhibition of tritiated cGMP breakdown by mant-cGMP was obtained at 7.5 +/- 1.4 micromolar (n = 6) and by unlabeled cGMP at 2.5 +/- 1.5 micromolar (n = 3). These values are similar to the published K_m for cGMP (5.5 ± 0.5 µM) [14].

mant-cGMP (1 mM) was tested for hydrolysis by PDE5 C domain (0.5 µM). The R_f values from the silica plate TLC for the pure standards and the nucleotides present in the

reaction mixture were determined: mant-cGMP, 0.66, and mant-5'-GMP, 0.40. R_f values from cellulose TLC were also determined (cellulose TLC allowed for detection of the unconjugated nucleotides): cGMP, 0.35; mant-cGMP, 0.76; 5'-GMP, 0.08; mant-5'-GMP, 0.40. Under these conditions 100% of mant-cGMP was converted to mant-5'-GMP. The combined results from K_i and TLC analysis indicated that mant-cGMP binds to and is hydrolyzed by PDE5 C domain.

Pre-steady-state Kinetics of mant-cGMP Interaction with Isolated Human PDE5 C domain

A complex increase in fluorescence was observed due to FRET ($\lambda_{excitation}$ = 295 nm and $\lambda_{emission}$ > 420 nm) when mant-cGMP was mixed with isolated PDE5 C domain in the presence of higher concentrations of Mg^{2+} (Figure 3a). Examples of fitting the data to three, four and five exponential terms are shown for the upper curve in Figure 3a for data obtained at 36mM Mg^{2+}. The data required five exponential terms to accurately fit the time course of fluorescence emission from 0.001 to 600 sec at each of the Mg^{2+} concentrations used. It is unusual to be able to resolve so many pre-steady-state steps in an enzymatic reaction. This can be done here because at 20°C the rates of each of the processes are >10 fold different from one another. Rate constants that are at least five-fold different are resolvable if they have the same amplitude sign. If the amplitudes have opposite signs then the resolvability is about a 50% difference. Dependence of the rates and amplitudes of the five exponential fits to the data are summarized in (Table 1). The data for each concentration of Mg^{2+} were then fit with a hyperbolic equation to determine the maximum rates, k_{imax}, of each step at saturating Mg^{2+} and the apparent affinity, K_{iMg} of each step (Figure 3b).The data are fit by three increases in FRET that occur with rate constants of 265 ± 37 s^{-1}, 23 ± 0.8 s^{-1}, and 0.24 ± 0.006 s^{-1}, a decrease with a rate constant of 0.03 ± 0.003 s^{-1}, and a final slow increase in fluorescence at 0.007 ± 0.0002 s^{-1}.

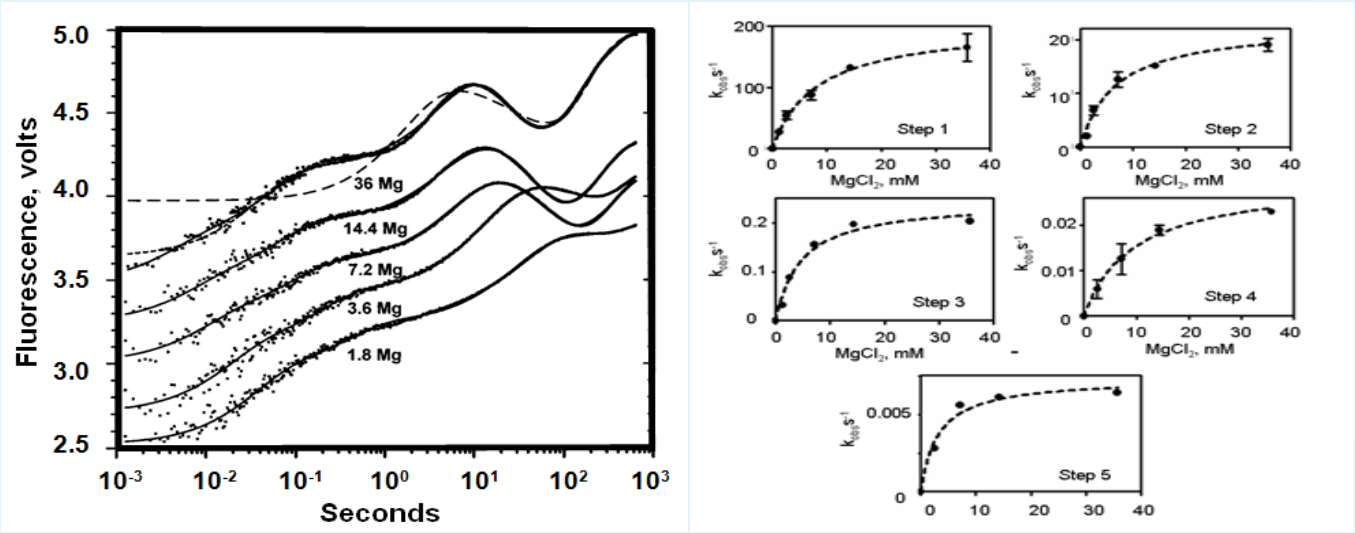

(A) **(B)**

Figure 3: Mg^{2+} dependence of FRET between mant-cGMP and PDE5 C domain. (A) Changes in FRET over 600 sec at 20 °C following mixing of isolated C domain (2.9 μM, final) with mant-cGMP (7.1 μM, final) and either 2, 5, 10, 20, or 50 mM $MgCl_2$ in 50 mM Tris-HCl, pH 8.0 $\lambda_{excitation}$ = 290 nm, $\lambda_{emission}$> 420 nm. Curves are displaced by 0.25 volt for clarity. The solid lines represents a five-exponential fit of $F(t) = \sum A(i)e^{-kit} + C$ at indicated concentrations of Mg^{2+}. The dotted line is a four exponential fit and the dashed line is a three exponential fit to the data derived from the experiments performed at 36 mM Mg^{2+}. (B)The dependence of the rate constants measured in (A) upon Mg concentrations were fit to a hyperbolic equation:

$Kn = Kn\,max/(1+[KMg]/[Mg])$. The rate and amplitudes of the exponential fits and secondary hyperbolic fits are summarized in Table 1.

Step(n)	Constant	Mg^{2+}					K_{nMg}	K_{nmax}
		1.8 mM	3.6 mM	7.2 mM	14.4 mM	36.0 mM	mM	s^{-1}
1	k_1 (s^{-1})	29.2	57.9	105	138	185	8 ± 2	265 ± 20
	A_1 (volts)	-0.423	-0.384	-0.279	-0.247	-0.269		
2	k_2(s^{-1})	2.63	5.42	10.3	15.3	18.9	7 ± 1	23 ± 2
	A_2(volts)	-0.289	-0.336	-0.327	-0.338	-0.478		
3	k_3(s^{-1})	0.038	0.093	0.16	0.19	0.2	5 ± 1	0.24 ± 0.02
	A_3(volts)	-0.5	-0.693	-0.661	-0.728	-1.126		
4	k_4(s^{-1})	0.0015	0.006	0.013	0.0194	0.023	10 ± 3	0.030 ± 0.004
	A_4(volts)	1.61	1.085	3.36	1.2	1.25		
5	k_5(s^{-1})	0.001	0.0031	0.0052	0.0057	0.0062	3 ± 1	0.0073 ± 0.0005
	A_5(volts)	-1.48	-1.104	-3.36	-0.969	-1.042		

Table 1: Stopped-Flow FRET Analysis of mantcGMP Interaction With the PDE5 Isolated C Domain Reveals Five Distinct Mg^{2+}-dependent Rates.

The parameters from fitting the FRET signals of mant-cGMP binding isolated PDE5 C domain at each Mg^{2+} concentration (Figure 3) to 5 exponential terms using equation 2 are shown in the left hand columns. The Mg^{2+} dependence of each rate parameter, k_n, was then fit to hyperbolic equation $k_n = k_{nmax}/ (1+K_{nMg}/ [Mg])$. The values for k_{nmax} and K_{nMg} are shown in the right two columns.

The three initial processes associated with increases in fluorescence suggested a sequence of conformational changes that occur following binding of mant-cGMP to the C domain prior to its hydrolysis and dissociation (the decrease in fluorescence) of the reaction product. Our results using HPLC showed a slow isomerization of the product with a similar time course to that of the final fluorescence increase (data not shown). Although other conclusions are possible, we interpret this as the 2' to 3' position isomerization of the mant group on the ribose-phosphate moiety of the analog product, 2'-mant-5'-GMP, followed by binding of 3'-mant-5'-GMP to the C domain to produce the final increase in fluorescence.

When PDE5 C domain was mixed with varying concentrations of mant-cGMP at 20°C under the same experimental conditions used in Figure 3, none of the five steps had rates that were dependent on mant-cGMP concentration (data not shown). Possible explanations for this were that at 20°C: a) mant-cGMP binding to the C domain occurs very rapidly during the "dead-time" required for mixing in the stopped-flow cell, or b) the concentration dependence was of insufficient magnitude to allow observation of such a rapid process. However, at 4 °C concentration dependence of the rate of the first fluorescent step upon mant-cGMP was observed and fit to a second order rate constant of 2.4 x 10^7 $M^{-1}s^{-1}$ (Figure 4).

A dissociation rate of 164 s^{-1} of mant-cGMP dissociation from the C domain was derived from the intercept. The rates of the association and dissociation measured could be used to calculate a dissociation constant of the initial enzyme-substrate complex at 4°C, K_S = 6.8 μM (equation 3).

$$K_s = k_{-1} / k_1 \qquad (3)$$

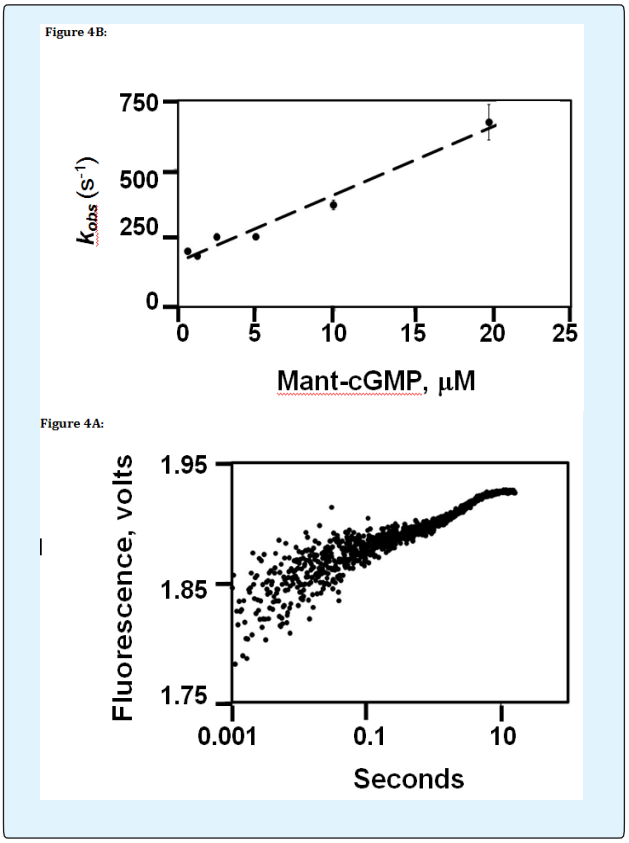

Figure 4: Dependence of the rates of mant-cGMP binding to isolated PDE5 C domain on mant-cGMP concentration at 4°C. Rate constants were measured following single-mixing of PDE5 C domain and mant-cGMP. Final concentrations in the stopped-flow cell for each rate (k_{obs}) determination were 1.2 μM C domain and the indicated concentration of mant-cGMP in 36 mM $MgCl_2$,20 mM Tris, 50 mM NaCl, pH 7.5. *A)* Data used to calculate the rate of 20 μM mant-cGMP binding to isolated PDE5 C domain. *B*) The line fit through the data shown in A corresponds to a second order rate constant of 2.4 x 10^7 M^{-1} s^{-1} and a y-intercept of 164s^{-1}. Observed rates are the mean ± S.E.M. of the results, n = 3

The highest Mg^{2+}concentration tested (36 mM) in the stopped-flow experiments was 3.6 times higher than that used in standard PDE assays (10 mM), so the Mg^{2+}effect on C domain steady-state kinetics was also assessed in a standard PDE assay. This was done using saturating substrate, 20 μM cGMP, and varying concentrations of $MgCl_2$ (0-10 mM). Under these conditions PDE catalytic activity increased with increasing concentrations of $Mg^{2+}$and plateaued at ~5 mM Mg^{2+} with a measured activation constant (K_a) of 1.0 mM Mg^{2+} (Figure 5). Thus, under both steady-state and pre-steady-state conditions the C domain activity was Mg^{2+}-dependent and required Mg^{2+} in the millimolar range.

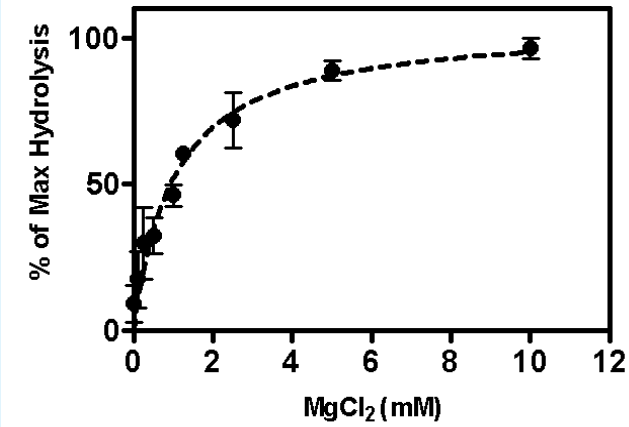

Figure 5: Mg^{2+} dependence of steady-state hydrolysis of cGMP by isolated PDE5 C domain. Hydrolysis of cGMP measured at 30 °C in the standard PDE assay containing final concentrations of 50 mM Tris-HCl, pH 7.5, 0.3 mg/ml bovine serum albumin, 10 nM C domain, and 20 μM [^{3}H]cGMP and the indicated $MgCl_2$ concentration in a final volume of 50 μl, as described in Experimental Procedures. Catalytic activity is expressed as % of maximum activity measured in a given assay. The calculated K_a = 1 mM $MgCl_2$. Less than 25% of total [^{3}H]cGMP was hydrolyzed in each determination. Rate at 10mM $MgCl_2$ was taken as 100%. Data reflect mean ± S.E.M of the results, n = 3.

The dissociation rate of 2'-mant-5'-GMP from C domain was directly measured by both double-mixing and single-mixing experiments. In the double-mixing experiment mant-cGMP was mixed with C domain for 20 sec, followed by mixing with excess cGMP (1 mM) and monitoring the time-dependent decline in fluorescence intensity (Figure 6A). The decrease in fluorescence using this approach fit a single exponent with a rate of 0.5s^{-1} at 20°C. Alternatively, single-mixing experiments were done by incubating mant-3',5'-GMP with C domain for 5 min to allow for complete hydrolysis before loading the sample into the stopped-flow apparatus and mixing the C domain-mant-3',5'-GMP complex with 2 mM cGMP at either 4 °C or 20 °C. The observed rates were 0.11 s^{-1} at 4 °C (Figure 6B) and 0.52 s^{-1} at 20°C (not shown).

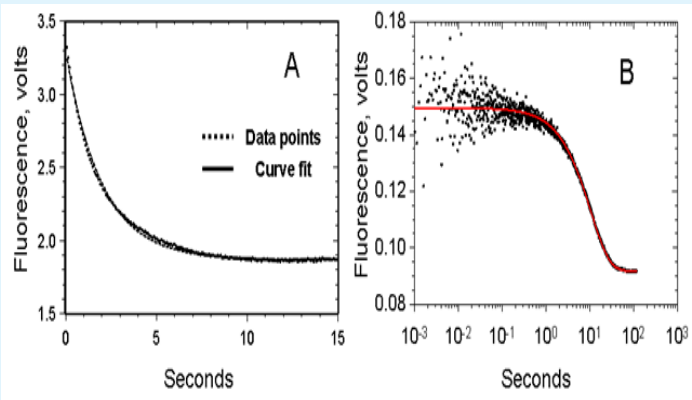

Figure 6: Dissociation rate of 2'-mant-5'-GMP from the isolated PDE5 C domain.

A) Double-mixing experiments to determine the rate of 2'-mant-5'-GMP dissociation from C domain complex intermediates were done by mixing 4.5 μM PDE5 C domain with 8.1 μM 2'-mant-cGMP, incubating for 20 sec in delay line, followed by mixing with 1 mM cGMP in stopped-flow cell. Final concentrations were 1 μM cGMP, 1.8 μM mant-cGMP and 556 uM cGMP.

B) Single-mixing determination of 2'-mant-5'-GMP dissociation from C domain was done by first incubating PDE5 (18 μM) with a mixture of 2'-mant-5'-GMP and 3'-mant-5'-GMP isomers (18 μM) on ice for 5 min, loading the mixture into stopped-flow syringe A and mixing with 2.8 mM cGMP. Final

concentrations in the stopped-flow cell were 4 μM PDE5, 4 uM mant-5'-GMP and 2 mM cGMP. The data were fit to single exponential curves with rates of 0.52 s^{-1} at s^{-1} 20°C (A) and 0.1 s^{-1} at 4°C (B).

Dissociation rates of substrate and product from the PDE5 C domain were also determined at various times after mixing enzyme and substrate by double-mixing stopped-flow. In these experiments mant-cGMP was pre-mixed with C domain and after the desired reaction time dissociation of substrate/product was measured by chasing with cGMP (2 mM final in the stopped-flow cell) to prevent the rebinding of mant-nucleotide (substrate or product) to the enzyme. The observed decrease in fluorescence emission in these experiments was due to loss of FRET between mant-nucleotide and C domain when the mant-nucleotide was replaced by cGMP. At 20°C and a final Mg^{2+} concentration of 36 mM, the fluorescence was fit to a single exponential curve with a rate of 0.45 ± 0.15 s^{-1} when measured after pre-mix times of greater than 2 sec, which is similar to the rate of mant-cGMP dissociation measured in Figure 6A. At shorter times, the decrease in fluorescence was more rapid than the mixing time of the stopped-flow and no signal was observed.

We also did a similar series of experiments at 4°C in which C domain was pre-mixed with mant-cGMP for 0.01 to 100 sec, and then mixed with cGMP (2 mM). When mant-cGMP and C domain were pre-mixed for 0.01 sec, a rapid dissociation rate (200 ± 50 s^{-1}) was measured (Figure 7A). This rate was in good agreement with the dissociation rate (164 s^{-1}) determined at 4 °C from the intercept of mant-cGMP binding experiments in Figure 4B. The measured dissociation rate was dependent on the pre-mix time (Figure 7). One hundred seconds after mixing, the rate of mant nucleotide dissociation was similar to the rate of mant-GMP dissociation from C domain as would expected after the substrate was all hydrolyzed. The data supported a model in which mant-cGMP initially binds with low affinity to the PDE5 C domain, but once bound, the rate of dissociation of the C domain-mant-cGMP complex progressively decreases with time. The decrease in fluorescence observed upon pre-mixing mant-cGMP and C domain at 4°C for 0.1 to 3 sec prior to addition of the cGMP chase was fit to single exponential curves with dissociation rates of 90-100 s^{-1}. For pre-mixing times >10 sec the data were fit to two exponential terms with a fast component from 40 to 120 s^{-1} and slow component from 0.11 to 0.39 s^{-1}. Both rates decreased as pre-incubation times of C domain with mant-cGMP were increased prior to additionof the cGMP chase (Figure 7B). The appearance of a slower dissociation rate following pre-mixing for 10 sec can be explained by the hydrolysis of mant-cGMP and subsequent dissociation of the product mant-GMP.

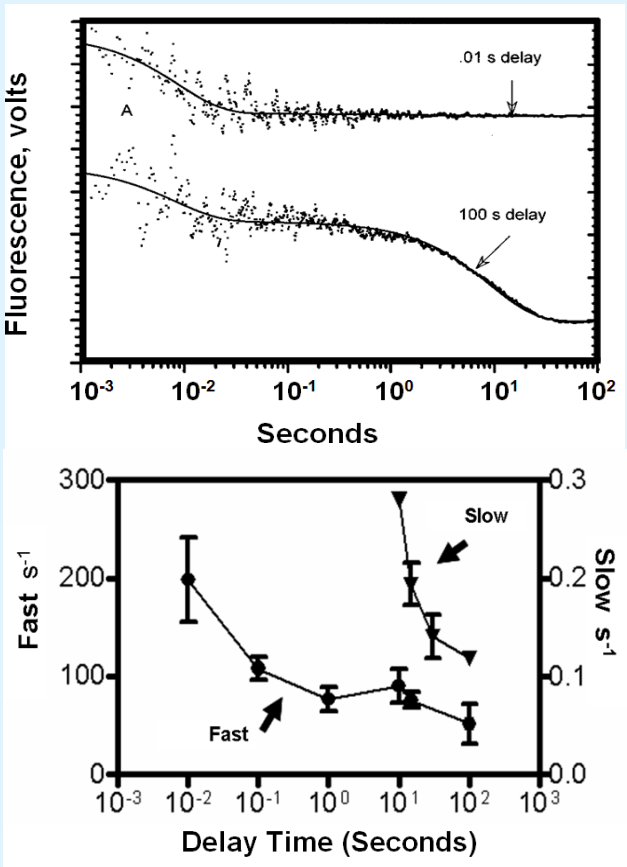

Figure 7: The time-dependent decrease in FRET between mant-cGMP and PDE after mixing with excess cGMP. PDE5 C domain (4 μM final in stopped-flow cell) and mant-cGMP (8 μM final) were pre-mixed, incubated for the indicated time in a delay line and then mixed with cGMP (2 mM final). Data for a 0.01 sec delay (upper curve) are fit by a k_{obs} of 154 s^{-1} and the data obtained after a 100 sec delay (lower curve) by k_{obs} of 122 s^{-1} and 0.11 s^{-1}. The dependence of the rapid and slow rates upon the length of the delay time. Experimental conditions: 20 mM Tris-HCl, pH 7.5, 50 mM NaCl, 36 mM $MgCl_2$. Data points represent the mean ± S.E.M of the measured rate, *n* = 4.

The hydrolytic rate of mant-cGMP by PDE C domain was determined by quench-flow. mant-cGMP was mixed with enzyme, incubated for the indicated time, and the reaction was stopped by mixing with 30 mM KH_2PO_4 and 10 mM tetrabutyl ammonium hydroxide, pH 2.65, as described in Experimental Procedures. The time

dependence of hydrolysis is shown in (Figure 8). The mant-cGMP hydrolytic step increased 5-fold from 0.0055 s^{-1} to 0.027 s^{-1} when $Mg^{2+}$was increased from 3.6 mM to 36 mM. The hydrolytic rate measured here was similar to the rates, 0.023s^{-1}, measured for Step 4 (fluorescence decrease) by stopped-flow with 3.6 and 36 mM $MgCl_2$ (Figure 3 and Table 1). Together these data indicated that Step 4 in Figure 3 is: a) limited by the hydrolysis of mantcGMP and b) is Mg^{2+}-concentration dependent. A more rapid rate of hydrolysis, 7.4 s^{-1}, for cGMP measured by quench-flow (data not shown) was similar to values obtained by steady state determinations [15].

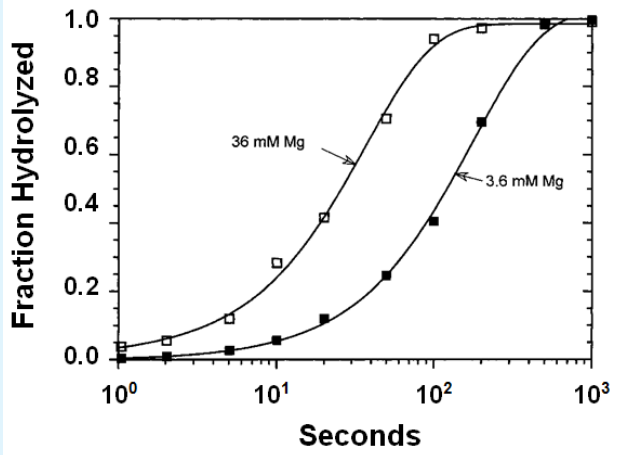

Figure 8: Quench-flow measurement of the time course of mant-cGMP hydrolysis. mant-cGMP hydrolysis rate was determined by measuring the appearance of mant-5'-GMP by HPLC (described in "Experimental Procedures"). Final concentrations for each time point were 2.5 μM C domain and 1.25 uM mant-cGMP. Experimental conditions were either 3.6 mM (□) or 36 mM $MgCl_2$ (■) in 20 mM Tris-HCl, at pH 7.5, 50 mM NaCl. The solid lines represent a single-exponential fit with a $k_{hydrolysis}$ of 0.0055 s^{-1} at 3.6 mM $MgCl_2$ and 0.027 s^{-1} at 36 mM $MgCl_2$.

Discussion

This is the first pre-steady-state study of the catalytic mechanism of any class I cyclic nucleotide PDE. Use of the isolated PDE5 C domain simplifies interpretation of results since in the absence of the regulatory domain the catalytic site is the only site of the enzyme that binds cGMP, cGMP analogs, or products. Furthermore, the k_{cat} and K_m for the PDE5 C domain approach the values for those of the holoenzyme [4,16], indicating that the salient features of the formation of the hydrolytic process are maintained.

Mant-cGMP is a useful tool to study the catalytic mechanism of PDE5; PDE5 C domain binds mant-cGMP with an affinity that is comparable to that of cGMP, although the rate of hydrolysis is ~200 fold slower. Published reports show that PDE1 and PDE6 also have much slower rates of hydrolysis for mantcAMP or mant-cGMP than for the respective unconjugated nucleotides, but the mant-cyclic nucleotides have similar affinities to those of unmodified cyclic nucleotide [3]. Mant is conjugated to the 2'-position of the ribose of cGMP (Figure 1). Analog studies have shown that the 2'-hydroxyl in cGMP does not contribute significantly to affinity of cGMP for the PDE5 catalytic site [11,16]. Thus, it is not surprising that the affinity of PDE5 C domain for mant-cGMP is similar to that of unmodified cGMP. Mant-analogs allow for FRET analysis, which provides a direct measure of substrate/product interactions with the C domain and cannot be done with unmodified cGMP.

While steady-state kinetic measurements are important in characterizing an enzyme, they are limited in providing detailed mechanistic information regarding substrate conversion to product in the active site [18]. Following rapid binding of mant-cGMP, stopped-flow analysis by FRET reveals four Mg^{2+}-dependent increases in fluorescence. The rates of all four of these steps are mant-cGMP concentration-independent at 20°C and concentration-dependent substrate binding can only be observed at 4°C. The two steps following binding of mant-cGMP are conformational changes that precede hydrolysis of the nucleotide followed by the dissociation of product, mant-5'-GMP. The multi-step increases in energy transfer between C domain tryptophan(s) and mant-cGMP suggest formation of increasingly tighter enzyme-substrate complexes. The equilibrium constants for each of the increases in FRET that are detected (K_2 and K_3 from Steps 2 and 3) must be favorable ($K_{eq} \geq 1$) or they would not be observed. An alternative analysis of the fluorescence data is to globally fit it to a five-step mechanism (5 equilibria and 10 rate constants) at each Mg^{2+} concentration. (See Supplemental Information).

The rates for the 5 steps are kinetically well separated, as each step is slower than the preceding step by at least one order of magnitude. Under the same conditions, the rate of Step 4 (k_4= 0.023 s^{-1}) is similar to the mant-cGMP hydrolytic rate ($k_{hydrolysis}$ = 0.027 s^{-1}) determined by quench-flow analysis (Figure 8). The kinetic data show that Step 4 is rate-limiting for the hydrolysis of mant-cGMP followed by the more rapid dissociation of mant-5'-GMP from the enzyme (k_{-P} = 0.5 s^{-1}). Step 5, which occurs

subsequent to dissociation of mant-5'-GMP, is slower than the steady state rate and therefore must be "off pathway". Mg^{2+} functions as an activator of PDE5 and all five steps measured in Figure 3a increase with Mg^{2+} concentration with K_{Mg++} values between 3 and 8 mM. Full activation would require Mg^{2+} higher than the published concentration of free Mg^{2+} in a smooth muscle cell [~1 mM] [19]. It seems unlikely that the amino-terminal regulatory region of PDE5, which is absent in the isolated C domain used here, is important for modulating PDE5 affinity for Mg^{2+} since PDE5 C domain affinity for Mg^{2+} (1 mM, Figure 5) is comparable to that of PDE5 holoenzyme using cGMP as a substrate [20]. It is possible that Mg^{2+} is not the preferred cation for PDE5. Several other cations, including Zn^{2+}, Co^{2+} and Mn^{2+}, have been shown to have substantially higher affinity than Mg^{2+} for the holoenzyme, and to promote PDE5 activity similar to that of Mg^{2+} [21]. However, affinities for Mg^{2+} measured using both steady-state (1 mM, Figure 5) and pre-steady-state (3-8 mM, Table 1) kinetics are in the same order of magnitude as found in cells.

The results presented here support a mechanism in which mant-cGMP rapidly binds to the PDE5 active site in the presence of Mg^{2+} (Figure 9). Figure 9 depicts a more complex pathway than the minimal mechanism of an enzyme catalyzed reaction (E + S ⇄ E-S ⇄ E-P ⇄ E +P). In Figure 9 the cyclic nucleotide within the catalytic site undergoes sequential conformational changes to ES' and ES'' that occur at distinct rates and ultimately result in hydrolysis of the cyclic nucleotide phosphodiester bond followed by product release. The initial enzyme substrate complex undergoes two Mg^{2+}-dependent conformational changes (steps 2 and 3 in Figure 9) that lead to formation of a high-affinity enzyme-substrate complex (ES''). The rate limiting hydrolytic step 4 is followed by more rapid dissociation of the reaction product, mant-GMP.

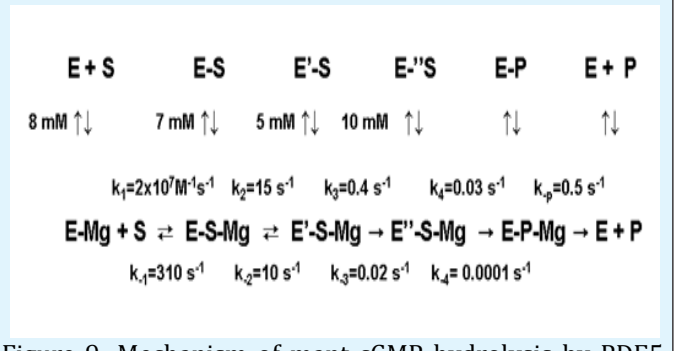

Figure 9: Mechanism of mant-cGMP hydrolysis by PDE5 isolated C domain. Experimental conditions: 36 mM $MgCl_2$, 20 mM Tris-HCl, pH 7.5, 50 mM NaCl at 20°C except for k_1 and k_{-1}, which were estimated by global fitting (Table SI). After substrate binding PDE5 C domain undergoes two conformational changes (k_2 and k_3) followed by hydrolysis (k_4) and dissociation of product 2'-mant-5'-GMP (k_{-P}). The rate constants were obtained by extrapolation to saturating Mg^{2+}. Abbreviations denote: mant-cGMP = S, PDE5 C domain = E, 2'-mant-5'-GMP = P, sequential conformational states of E'-S and E''-S are sequential enzyme substrate complexes.

A recent report by Liu et al. determined that for PDE9, substrate binding and hydrolysis are fast and that the rate-limiting step is dissociation of hydrolytic product, 5'-GMP [22]. This conclusion was based upon the observation that hydrolysis of substoichiometric quantities of cGMP was >98% complete in 10 sec (i.e. k ≥ 0.3 s^{-1}) but the steady state rate observed with excess substrate was only 0.02 s^{-1}. These results indicate that substrate binding and hydrolysis are not rate-limiting for PDE9, but the rate of product dissociation was not directly measured. The results of our studies of PDE5 using the substrate analog mant-cGMP indicate that the hydrolytic step is rate-limiting and product dissociation at least 10 fold more rapid than hydrolysis. It would not be surprising if the rate-limiting step in catalysis differs among PDE families since there is a large (>8000-fold) variation in the steady-state rates of different PDEs [23]. This possibility is more plausible when one considers known factors that influence the catalytic rates of various PDEs; these include

a) Different specificities among PDEs for support of catalysis by particular divalent cations [21,24-26].
b) Potential differences in positioning of the cyclic phosphate moiety in relationship to the catalytic machinery (due to preference for either the *anti* or *syn* conformer of the cyclic nucleotide substrate) [10,27,28].
c) Differences in topography of the catalytic sites [29].
d) Regulatory influences of step(s) in the catalytic process.

The hydrolytic rate of the isolated PDE5 C domain for cGMP is 7.4s^{-1} at 20°C. The dissociation rate for cGMP is expected to approximate that of mant-cGMP (~300 s^{-1} at 20°C) since both molecules have similar affinities for the C domain. Thus, ~1 cGMP molecule is hydrolyzed per ~50 cGMP molecules that bind to the catalytic site; this means that the initial binding of cGMP is relatively weak and reversible. Factors (e.g. phosphorylation, binding of regulatory ligands to the allosteric site) that increase the

affinity and/or hydrolytic rate (the rate-limiting step) for cGMP may significantly increase PDE5 catalytic efficiency (k_{cat}/K_m). Existence of a multi-step catalytic process for PDE5 implies that regulation of this enzyme could occur at one or more steps. Several different modes of regulation of PDE5, e.g. phosphorylation, allosteric regulation, and substrate effect, are well-known [30], but whether or not they modulate the same step(s) of the catalytic process has not been studied. If genetic diseases involving PDE5 mutations that affect catalysis are identified, it would be important to identify the steps modified by this alteration.

Data presented here enhance our understanding of the PDE5 catalytic mechanism and show that hydrolysis is the rate-limiting step of PDE5 for breakdown of mant-cGMP. It will be of interest to determine if elements of the catalytic mechanism identified here, i.e. multi-step conformational changes with Mg^{2+}-dependent rates, and/or a rate-limiting step of substrate hydrolysis, occur in other class I PDEs and to identify differences among the mechanisms of the 11 PDE families that could account for the wide range of differences in their catalytic rates.

Acknowledgement

Research supported by NIH DK40029 (JC and SF), Stipend support for GZM from Vascular Biology Training Grant NIH NHBLI 5 T32 HL07751 (R. Hoover), NIH GM 59791 (HK), and NIH HL084604 (HW).

References

1. Cote RH (2006) Photoreceptor phosphodiesterase (PDE6): a G-protein-activated PDE regulating visual excitation in rod and cone photoreceptor cells. Cyclic Nucleotide Phosphodiesterases in Health and Disease. Beavo J, Francis SH, Houslay MD (Eds), CRC Press, USA, pp. 165-193.

2. Cawley SM, Sawyer CL, Brunelle KF, van der Vliet A, Dostmann WR (2007) Nitric Oxide-Evoked Transient Kinetics of Cyclic GMP in Vascular Smooth Muscle Cells. Cell Signal 19(5): 1023-1033.

3. Hiratsuka T (1982) New Fluorescent Analogs of cAMP and cGMP Available as Substrates for Cyclic Nucleotide Phosphodiesterase. J Biol Chem *257*:13354-13358.

4. Huai Q, Liu Y, Francis SH, Corbin JD, Ke H (2004) Crystal Structures of Phosphodiesterases 4 and 5 in Complex with Inhibitor 3-Isobutyl-1-Methylxanthine Suggest a Conformation Determinant of Inhibitor Selectivity. J Biol Chem 279(13): 13095-13101.

5. Blount MA, Zoraghi R, Hengming Ke, Bessay EP, Corbin JD, et al. (2006) A 46-Amino Acid Segment in Phosphodiesterase-5 GAF-B Domain Provides for High Vardenafil Potency Over Sildenafil and Tadalafil and is Involved in Phosphodiesterase-5 Dimerization. Mol Pharmaco 70(5): 1822-1831.

6. Thomas MK, Francis SH, Corbin JD (1990) Characterization of a Purified Bovine Lung cGMP Binding cGMP Phosphodiesterase. J Biol Chem 265(25): 14964-14970.

7. Cheng Y, Prusoff WH (1973) Relationship Between the Inhibition Constant (K1) and The Concentration of Inhibitor which Causes 50 Per Cent Inhibition (I50) of an Enzymatic Reaction. Biochem Pharmacol 22(23): 3099-3108.

8. Ni Q, Shaffer J, Adams JA (2000) Insights into Nucleotide Binding in Protein Kinase A Using Fluorescent Adenosine Derivatives. Protein Sci 9(9): 1818-1827.

9. Woodward SK, Eccleston JF, Geeves MA (1991) Kinetics of the Interaction Of 2'(3')-O-(N-Methylanthraniloyl)-ATP With Myosin Subfragment 1 and Actomyosin Subfragment 1: Characterization Of Two Acto-S1-ADP Complexes. Biochemistry 30(2): 422-430.

10. Thomas MK, Francis SH, Beebe SJ, Gettys TW, Corbin JD (1992) Partial Mapping of Cyclic Nucleotide Sites and Studies of Regulatory Mechanisms of Phosphodiesterases Using Cyclic Nucleotide Analogues. Adv Second Messenger Phosphoprotein Res 25: 45-53.

11. Johnson JD, Walters JD, Mills JS (1987) A Continuous Fluorescence Assay for Cyclic Nucleotide Phosphodiesterase Hydrolysis of Cyclic GMP. Anal Biochem 162(1): 291-295.

12. Grewal J, Karuppiah N, Mutus B (1989) A Comparative Kinetic Study of Bovine Calmodulin-Dependent Cyclic Nucleotide Phosphodiesterase Isozymes Utilizing cAMP, cGMP and Their 2'-O-Anthraniloyl-,2'-O-(N-methylanthraniloyl)-

derivatives as Substrates. Biochem Int 19(6): 1287-1295.

13. Brown RL, Stryer L (1989) Expression in Bacteria of Functional Inhibitory Subunit of Retinal Rod cGMP Phosphodiesterase. Proc Natl Acad Sci USA 86(13): 4922-4926.

14. Wang H, Liu Y, Huai Q, Cai J, Zoraghi R, et al. (2006) Multiple Conformations of Phosphodiesterase-5: Implications For Enzyme Function and Drug Development. J Biol Chem 281(30): 21469-21479.

15. Fink TL, Francis SH, Beasley A, Grimes KA, Corbin JD (1999) Expression of an active, monomeric catalytic domain of the cGMP-binding cGMP-specific phosphodiesterase (PDE5). J Biol Chem 274(49): 34613-34620.

16. Francis SH, Thomas MK, Corbin JD (1990) Cyclic Nucleotide Phosphodiesterases: Structure, Regulation and Drug Action. Beavo J, Housley MD (Eds), John Wiley and Sons, US, pp 117-140.

17. Heeley DH, Belknap B, White HD (2006) Maximal Activation of Skeletal Muscle Thin Filaments Requires Both Rigor Myosin S1 and Calcium. J Biol Chem 281(1): 668-676.

18. Grant BD, Adams JA (1996) Pre-steady-state Kinetic Analysis of cAMP-dependent Protein Kinase Using Rapid Quench Flow Techniques. Biochemistry 35(6): 2022-2029.

19. Tashiro M, Konishi M (1997) Basal Intracellular Free Mg^{2+} Concentration in Smooth Muscle Cells of Guinea Pig Tenia Cecum: Intracellular Calibration of the Fluorescent Indicator Furaptra. Biophys J 73(6): 3358-3370.

20. Francis SH, Turko IV, Grimes KA, Corbin JD (2000) Histidine-607 and Histidine-643 Provide Important Interactions for Metal Support of Catalysis in Phosphodiesterase-5. Biochemistry 39(31): 9591-9596.

21. Francis SH, Colbran JL, McAllister-Lucas LM, Corbin JD (1994) Zinc Interactions and Conserved Motifs of the cGMP-Binding cGMP-Specific Phosphodiesterase Suggest that it is a Zinc Hydrolase. J Biol Chem 269(36): 22477-22480.

22. Liu S, Mansour MN, Dillman KS, Perez JR, Danley DE, et al. (2008) Structural Basis for the Catalytic Mechanism of Human Phosphodiesterase 9. Proc Natl Acad Sci USA 105(36): 13309-13314.

23. Bender AT, Beavo JA (2006) Cyclic Nucleotide Phosphodiesterases: Molecular Regulation to Clinical Use. Pharmacol Rev 58(3): 488-520.

24. Cheung PP, Xu H, McLaughlin MM, Ghazaleh FA, Livi GP, et al. (1996) Human platelet cGI-PDE: expression in yeast and localization of the catalytic domain by deletion mutagenesis. Blood 88(4): 1321-1329.

25. Fisher DA, Smith JF, Pillar JS, St Denis SH, Cheng JB (1998) Isolation and characterization of PDE9A, a novel human cGMP-specific phosphodiesterase. J Biol Chem 273(25): 15559-15564.

26. Michaeli T (2006) Cyclic Nucleotide Phosphodiesterases in Health and Disease. Beavo J, Francis S, Houslay MD (Eds), CRC Press, USA, pp. 195-203.

27. Beltman J, Becker DE, Butt E, Jensen GS, Rybalkin SD, et al. (1995) Characterization of cyclic nucleotide phosphodiesterases with cyclic GMP analogs: topology of the catalytic domains. Mol Pharmacolgy 47(2): 330-339.

28. Butt E, Beltman J, Becker DE, Jensen GS, Rybalkin SD, et al (1995) Characterization of Cyclic Nucleotide Phosphodiesterases with Cyclic AMP Analogs: Topology of The Catalytic Sites and Comparison With Other Cyclic AMP-Binding Proteins. Mol Pharmacol 47(2): 340-347.

29. Ke H, Wang H (2006) Structure, catalytic mechanism, and inhibitor selectivity of cyclic nucleotide phosphodiesterases. Cyclic Nucleotide Phosphodiesterases in Health and Disease. Beavo J, Francis SH, Houslay MD (Eds.), CRC Press, USA, pp. 607-625.

30. Corbin JD, Turko IV, Beasley A, Francis SH (2000) Phosphorylation of Phosphodiesterase-5 by Cyclic Nucleotide-Dependent Protein Kinase Alters its Catalytic and Allosteric cGMP-Binding Activities. Eur J Biochem 267(9): 2760-2767.